

# An Optimal Energy Management Strategy for Standalone DC Microgrids

Jis Sunny C

M. Tech,

Dept. of Electrical & Electronics Engg.  
Thejus Engineering College  
Thrissur, Kerala

Jyothi P Thomas

Asst. Prof,

Dept. of Electrical & Electronics Engg.  
Thejus Engineering College  
Thrissur, Kerala

**Abstract**— The energy management strategies are becoming vital for proper power sharing and voltage regulation purposes now a days. The usual energy management methods mainly depends up on MPPT techniques and sometimes based on batteries in case of excess or deficit of energy. For the constant voltage and current charging of batteries and also to increase their life span, a flexible energy management method is to be introduced. So here, a synchronized energy management strategy is offered with the help of “Nonlinear Model Predictive Control Algorithms (NMPC)”. This method makes the wind turbine and a photovoltaic array of a standalone DC microgrid as controllable power generators by adjusting the switching duty cycles of converters and the pitch angle of wind turbine. The technique is developed as an online NMPC based algorithms. By applying this proposed method to a standalone dc microgrid, the controller can realize the constant current and voltage charging of battery cells. The changing load demands can be accurately shared between corresponding generators. Also the voltage of DC bus can be easily regulated with in a specific range.

**Keywords**— *Battery life management , MPPT (Maximum Power Point Tracking) , NMPC (Nonlinear Model Predictive Control), Controllable Generators , Voltage regulation.*

## I. INTRODUCTION

In the future, distribution networks will consist of several interconnected smart microgrids that have the capability to locally generate, consume, and store energy[1]. A microgrid can be operated as an extension of a main power grid, i.e., in grid-connected mode , or as a standalone network without a connection to the main power grid. The most common applications of standalone dc microgrids are in the field of avionic, marine , industrial areas , as well as in electrification of remote areas. In the case of ac systems , the need of synchronization is very essential for several generators [2],[3]. The dc microgrids are more efficient than ac microgrids because the dc generators and storage batteries do not need ac-dc converters for being connected to dc microgrids [4],[1]. Voltage regulation, proper power sharing, and battery management are more severe in standalone dc microgrids that consist of only solar and wind energy sources and lead to the necessity of more developed control strategies.

The main control objective is to find out the stability of dc microgrid that can be obtained from the stability of dc bus voltage level [5],[6],[7]. The voltage level of grid-connected dc microgrids can be regulated by the use of grid voltage source converters (G-VSCs) [8],[9]. Battery banks are the

effective slack terminals for standalone dc microgrids [6] ; and their energy absorbing capacities are usually limited regarding a number of operational constraints. To regulate the voltage level of standalone dc microgrids, the works in [2] and [6] presents load shedding strategies for the insufficient power generation or energy storage. The works in [10]–[12],presents strategies that decrease the renewable power generations of standalone dc microgrids if the storage battery bank cannot absorb the excess generation. These curtailment strategies restrict the batteries charging rate by absorbing maximum power; however, the maximum charging current must also be limited. They do not curtail the power of each generator in proportion to its rating.

To prevent circulating currents between generators and overstressing conditions [13], load demands must be shared accurately between all slack DGs in proportion to their ratings [7], [14]. Standalone dc microgrids are usually located in areas where the power sharing between DGs can be easily managed by centralized algorithms that are less affected by two main issues: 1) the absolute voltage level of a standalone microgrid is shifted as the result of the load demand variation ; 2) batteries in charging mode are nonlinear loads causing distortions to the grid voltage.

The charging mode operation of batteries [19] are seriously affected by; 1) the internal resistance & hence power losses and thermal effects increase at high SOC levels; 2) supplying high charging currents, the batteries voltage quickly reach to the gassing threshold and 3) batteries cannot be fully charged with a constant high charging current. The work in [6] limits the maximum absorbed power by the batteries in order to protect them from being overcharged. The batteries can acts as nonlinear loads during the charging mode, but it can not necessarily limit the charging currents.

Depending upon the total power generation to the load demand ratio within a standalone DC microgrids, three cases are noticed; 1) When the power generation is higher than load demand,it leads batteries to be overcharged and bus voltage to rise, 2) Total power generation and total load demands are balanced,3)Load demand exceeds power generation causes the dc bus voltage to drop in the absence of any load shedding.

This paper mainly focuses on case 1 in which the generated power must be limited if it violates the charging rates of batteries or if batteries are fully charged. An energy management strategy (EMS) is introduced to address, as its main control objectives, three aforementioned issues

corresponding to the standalone dc microgrids; i.e., proportional power sharing, battery management and the dc bus voltage regulation. In addition to the different strategies available in literature in which renewable energy systems (RESs) always operate in their maximum power point tracking(MPPT) mode, the proposed multivariable energy management strategy uses a PV array and a wind turbine as controllable generators and curtails their generations if it is necessary. The proposed energy management technique is developed as an online novel Nonlinear Model Predictive Control (NMPC) strategy that continuously solves an optimal control problem (OCP) and then finds the optimum values of three switching duty cycles and the pitch angle of the wind turbine. It can simultaneously control these following three variables of the DC microgrids: i.e., 1) angular velocity and power coefficient of the wind turbine, 2) charging current of the battery bank, 3) operating voltage of the photo voltaic array. It is shown that, by introducing new available nonlinear

model optimization techniques and tools, the usual computational time to solve the resulting predictive control strategy is in permissible limit. Unlike dump load-based strategies that only protect the battery from overcharging, the proposed energy management strategy implements the constant voltage and constant current charging regime of batteries that helps to improve the batteries life span. Moreover, by the removal of dump loads, the overall installation cost can be reduced.

This paper is presented as follows: Section II describes the mathematical modelling of standalone dc microgrids. Section III presents the proposed energy management strategy as an optimal control problem which is realized as an NMPC-based strategy. Section IV presents and discusses the results obtained. The conclusion of the work is given in Section V.

## II. SYSTEM MODELLING

The Fig. 1 shows topology of a small-scale standalone dc microgrid usually used for remote applications. The wind turbine is connected to the electrical generator directly(direct-drive coupling) and thus it is more efficient and reliable. The variable speed operation is more suitable for the power management applications[21]. From the Fig.1, it can be seen that battery bank is connected to the dc bus through a dc-coupled structure, i.e.,through a bidirectional dc-dc converter, which is more reliable in terms of implementing different charging and discharging regimes despite more power losses [19]. The authors in paper [20] describes a mathematical model of standalone dc microgrids as hybrid differential algebraic equations.

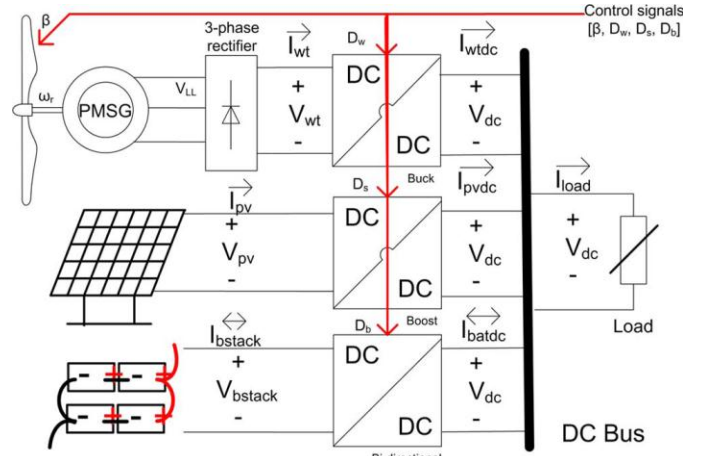


Fig. 1. Topology of a small-scale and standalone dc microgrid.

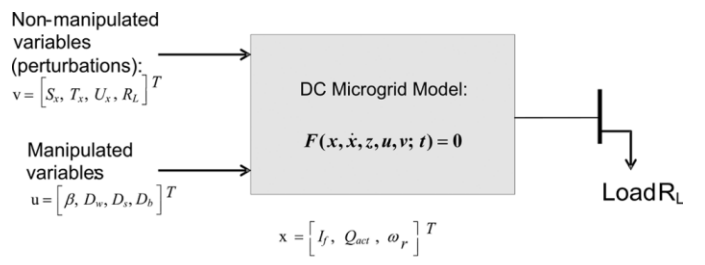


Fig. 2. Modified version of the system model in [20] for this paper.

Fig. 2 describes a modified version of the proposed dc microgrid model in [20]. Since this paper mainly focuses on the case

in which there is an excess power greater than or equal to the maximum possible absorbing rate of the storage battery bank, the hybrid nature of the battery bank operation is ignored for its simplicity. Here the differential and algebraic states are  $x$  and  $z$  respectively. Also the manipulated and non-manipulated control variables are  $u$  and  $v$  respectively. The following function is used to model the standalone dc microgrid in Fig. 1 as DAEs:

$$\mathcal{F}(x, \dot{x}, z, u, v) = \begin{bmatrix} f_1(x, \dot{x}, z, u, v) \\ f_2(x, \dot{x}, z, u, v) \\ \vdots \\ f_{24}(x, \dot{x}, z, u, v) \end{bmatrix} = 0 \quad (1)$$

where “F” is a set of implicit differential and algebraic functionals  $f_i$  for  $i \in \{1, 2, \dots, 24\}$ .

Here  $f_1$  and  $f_2$  are explained due to the fact that due to the fact that in standalone dc microgrids the sum of the generated, stored, and consumed energy is always equals to zero.

$$f_1 = V_{dc} (I_{pvdc} + I_{wtdc} + I_{batdc} - I_{load}), \quad (2a)$$

$$f_2 = V_{dc} - I_{load} R_L. \quad (2b)$$

### A . Wind Branch design

$$f_3 = C_{p,norm} - \frac{1}{C_{p,max}} \times (C_1 \left( \frac{C_2}{\lambda_i} - C_3 \beta - C_4 \right) \exp \left( -\frac{C_5}{\lambda_i} \right) + C_6 \lambda), \quad (3a)$$

$$f_4 = \lambda - \frac{Rad \times \omega_r}{U_x}, \quad (3b)$$

$$f_5 = \lambda_i - \left( \frac{1}{\lambda + 0.08\beta} - \frac{0.035}{\beta^3 + 1} \right)^{-1}, \quad (3c)$$

Where, ‘λ’ is the tip speed ratio and ‘β’ is the pitch angle.  $R_{ad}$  is the radius of the blades and  $C_{p,max}$  is the maximum achievable power coefficient at the optimum tip speed ratio of  $\lambda_{opt}$  [24].

The connected PMSG generator equations are given by :

$$f_6 = \frac{d\omega_r}{dt}(t) - \frac{1}{J}(T_e - T_m - F\omega_r), \quad (4a)$$

$$f_7 = -T_e \times \omega_r - I_{wt,dc} \times V_{dc}, \quad (4b)$$

$$f_8 = -T_m \times \omega_r - (C_{p,norm} \left( \frac{U_x}{U_{x,base}} \right)^3 P_{nom}). \quad (4c)$$

The energy management methods of microgrids should be capable of finding the dc bus voltage level deviation from its set point in about every 5–10 s [13]. The equation (4a) is the equation describing the angular velocity of the generator, equation (4b) is electromagnetic power and the equation (4c) shows that the PMSG is connected directly to turbine, which rotates at low speed [22]. ‘J’ is the shaft inertia in (Kg.m<sup>2</sup>) and ‘F’ is the combined viscous friction coefficient given in (N.m.s).

The average model of the buck converter can be replaced with the steady state conditions for the continuous conduction mode (CCM) [25] :

$$f_9 = V_{dc} - D_w V_{wt}, \quad (5a)$$

$$f_{10} = I_{wt} - D_w I_{wt,dc} \quad (5b)$$

where  $D_w$  is the switching duty cycle of the converter.

The average dc output voltage of the rectifier is given by  $V_{wt}$  and can be written as

$$V_{wt} = 1.35V_{LL} - \frac{3}{\pi}\omega_e L_s I_{wt} \quad (6)$$

The dc output current of the wind branch can be described by the following equation  $I_{wt,dc}$  :

$$f_{11} = I_{wt,dc} - \frac{\pi}{3P\omega_r L_s D_w} \left\{ \frac{1.35\sqrt{3}P\psi\omega_r}{\sqrt{2}} - \frac{V_{dc}}{D_w} \right\}. \quad (7)$$

### B . Battery Branch design

The battery bank charging operation consisting of  $N_{bat,p} \times N_{bat,s}$  batteries and is modeled using the following way (8): [26]

$$f_{12} = \frac{V_{bstack}}{N_{bats}} - V_0 + R_{bat} \frac{I_{bstack}}{N_{batp}} + \frac{P_1 C_{max}}{C_{max} - Q_{act}} Q_{act} + \frac{P_1 C_{max}}{Q_{act} + 0.1 C_{max}} I_f, \quad (8a)$$

$$f_{13} = \frac{dQ_{act}(t)}{dt} - \frac{1}{3600} \frac{I_{bstack}(t)}{N_{batp}}, \quad (8b)$$

$$f_{14} = \frac{dI_f}{dt}(t) + \frac{1}{T_s}(I_f - \frac{I_{bstack}}{N_{batp}}), \quad (8c)$$

$$f_{15} = V_{bstack} - \frac{V_{dc}}{1 - D_b}, \quad (8d)$$

$$f_{16} = I_{bstack} - (1 - D_b) I_{batdc}, \quad (8e)$$

$$f_{17} = SOC - \left\{ 1 - \frac{Q_{act}}{C_{max}} \right\} \quad (8f)$$

Where  $V_{bstack}$  is the voltage of the battery bank,  $I_{bstack}$  is the current of the battery bank and SOC is the ‘State Of Charge’ of the battery bank.

Other parameters are  $I_f$  which is the filtered value of the battery current with a constant time of  $T_s$  seconds,  $Q_{act}$  is the original battery capacity.

### C . Solar Branch

The following equations shows the characteristics of PV array consisting of  $N_{pv,p} \times N_{pv,s}$  photovoltaic modules:

$$f_{18} = I_{pv} - I_{ph} + I_0 \left\{ \exp \left( \frac{V_{pv} + \frac{N_{pv,s}}{N_{pv,p}} R_s I_{pv}}{n_d N_s} \frac{q \times N_{pv,s}}{K T_c} \right) - 1 \right\} + \frac{V_{pv} + \frac{N_{pv,s}}{N_{pv,p}} R_s I_{pv}}{\frac{N_{pv,s}}{N_{pv,p}} R_{sh}}, \quad (9a)$$

$$f_{19} = I_{ph} - N_{pv,p} \times \left( \frac{R_s + R_{sh}}{R_{sh}} I_{sc,stc} + k_I (T_c - T_{c,stc}) \right) \frac{S}{S_{stc}}, \quad (9b)$$

$$f_{20} = I_0 - N_{pv,p} \times \frac{I_{sc,stc} + k_I (T_c - T_{c,stc})}{\exp \left( \frac{V_{oc,stc} + k_V (T_c - T_{c,stc})}{n_d N_s} \frac{q}{K T_c} \right) - 1} \quad (9c)$$

Where  $I_{ph}$  is the photo current obtained and  $I_0$  is the diode reverse saturation current [28].  $R_s$  is the series equivalent resistance of PV module and  $R_{sh}$  is the resistance of parallel equivalent resistance of PV module.

The other parameters are given by :

q Charge of an electron ( $1.602 \times 10^{-19}$ )

K Boltzman constant ( $1.38 \times 10^{-23}$ )

$N_s$  No:of PV cells in series

$T_c$  PV cell temperature in (K)

$I_{s,stc}$  Short circuit current of PV module in (A)

$k_I$	Temperature coefficient of the SC current in ( $A/^\circ C$ )
$k_V$	Temperature coefficient of the OC voltage in ( $V/^\circ C$ )
$S$	Solar irradiance in ( $Wb/m^2$ )
$S_{stc}$	Solar irradiance at the STC ( $Wb/m^2$ )
$T_{c,stc}$	Cell temperature at STC (K)
$V_{oc,stc}$	OC voltage of PV module at STC (V)

The boost converter is replaced with the given steady state equations for CCM :

$$f_{21} = V_{pv} - (1 - D_s)V_{dc}, \quad (10a)$$

$$f_{22} = I_{pvdc} - (1 - D_s)I_{pv}. \quad (10b)$$

### III. CONTROLLER DESIGN

#### A) Optimal Control Problems (OCP) and Nonlinear Model Predictive Control (NMPC)

OCPs, as (11), makes use of the complete system model and can be represented by (11b), to find an optimal control law as  $u^*(.)$  and can define a certain number of equality and inequality constraints. The criterion is explained with a cost function  $J$  which consist of an Lagrangian term  $\mathcal{L}$  and the terminal cost term  $\mathcal{M}$ . Lagrangian term shows the cost function when time  $T$ . The equations (11d) and (11e) finds the final and initial constraints respectively which must be controlled by the optimal solution. Equation (11g) shows the box constraints on the states and control variables.

The optimal control law can be written as :

$$u^*(.) = \arg \min_{u(.)} J(x(t), z(t), u(t), T) :=$$

$$\int_t^{t+T} \mathcal{L}(x(\tau), z(\tau), u(\tau)) d\tau + \mathcal{M}(x(T), z(T)) \quad (11a)$$

$$\text{s.t.: } \mathcal{F}(x(t), \dot{x}(t), z(t), u(t), v(t)) = 0 \quad (11b)$$

$$\mathcal{H}(x(t), z(t), u(t)) \leq 0 \quad (11c)$$

$$\mathcal{R}(x(T), z(T)) = 0 \quad (11d)$$

$$x(t) = x_0, z(t) = z_0 \quad (11e)$$

$$\forall \tau \in [t, t+T] \quad (11f)$$

$$x(\tau) \in \mathcal{X}, z(\tau) \in \mathcal{Z}, u(\tau) \in \mathcal{U}. \quad (11g)$$

#### B) CONTROL SYSTEM

The following figure:3 shows the dc microgrid with proposed control system. It mainly focuses on the battery charging mode operation, thus only the boost side of the connected bidirectional converter is shown. The proposed optimal energy management method successively gets the estimated

system states, as inputs and then calculates the optimal solution for the problem as the output. The dc bus voltage level of the microgrid can be set externally and the developed controller can work as the secondary and primary levels of the hierarchical architecture [13].

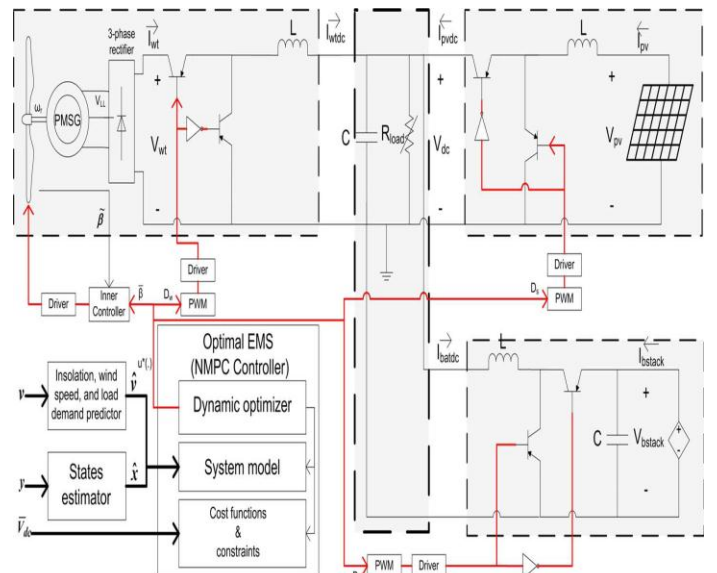


Fig. 3. Simplified view of the dc microgrid and the developed NMPC controller. The battery bank is assumed to work in charging mode.

The proposed predictive controller consists of three parts:

- 1) The dynamic optimizing part that can continuously solves an optimal control problem at each time  $h$ , defined in Table I;
- 2) The mathematical model of the system to find its operational behavior; and 3) The cost function constraints of the proposed optimal control problem. The optimum pitch angle  $\beta$  which is applied to an inner closed loop controller. The optimum values of the switching duty cycles are applied to the pulse width modulators (PWM) of the dc-dc converters.

The following Table I shows the design parameters and computational times of the developed predictive controller :

Parameter Name	Parameter Value
Prediction horizon $T$ (sec)	10
Sampling time $h$ (sec)	5.0
No. of the discretization samples $N$	2
$\bar{V}_{dc}(V)$	48.0
Average Computational Time (sec)	2.066
Minimum Computational Time (sec)	0.628
Maximum Computational Time (sec)	3.565

TABLE 1 : DESIGN PARAMETERS AND THE COMPUTATIONAL TIME OF THE DEVELOPED NMPC CONTROLLER

$$J(x(n), z(n), u(n), N) := \sum_{k=n}^{n+N} \left\{ \beta_1 \left\| \frac{1}{I_c} \left( \frac{I_{bstack}(k)}{N_{batp}} - \bar{I}_c \right) \right\|_2 + \beta_2 \left\| \frac{V_{dc}(k) - \bar{V}_{dc}}{\bar{V}_{dc}} \right\|_2 \right\} + \left\{ \beta_1 \left\| \frac{1}{I_c} \left( \frac{I_{bstack}(N)}{N_{batp}} - \bar{I}_c \right) \right\|_2 + \beta_2 \left\| \frac{V_{dc}(N) - \bar{V}_{dc}}{\bar{V}_{dc}} \right\|_2 \right\} \quad (14a)$$

1) Control Objectives:

The main control objectives are regulation of dc bus voltage, proportional power sharing between loads, and implementing the constant voltage and constant current charging of batteries, are explained by the following equations (12), (13) & (14):

$$f_{23} = \alpha_1 - (V_{dc} - \bar{V}_{dc}). \quad (12)$$

The deviation of the dc bus voltage level  $V_{dc}$  from the specified set point is defined by a slack variable  $\alpha_1$  in the above equation (12).

$$f_{24} = \alpha_2 - \left\{ \frac{I_{wtdc} V_{dc}}{P_{wt,nom}} \left( \frac{U_{x,base}}{\max(U_x, U_{x,base})} \right)^3 - \frac{I_{pvdc} V_{dc}}{P_{pv,nom}} \frac{S_{x,base}}{\max(S_x, S_{x,base})} \right\}. \quad (13)$$

The permissible variation from the optimal power sharing is given in above equation (13) in terms of  $\alpha_2$ . The power that is generated is normalized with respect to the wind speed and Irradiance values. i.e.,  $U_x$  and  $S_x$ .

The constant voltage and constant current charging of battery banks are explained by the following two equations (14a) and (14b):

$$J(x(n), z(n), u(n), N) := \sum_{k=n}^{n+N} \left\{ \beta_3 \left\| \frac{V_{bstack}(k) - N_{bats} V_{gas}}{N_{bats} V_{gas}} \right\|_2 + \beta_4 \left\| \frac{V_{dc}(k) - \bar{V}_{dc}}{\bar{V}_{dc}} \right\|_2 \right\} + \left\{ \beta_3 \left\| \frac{V_{bstack}(N) - N_{bats} V_{gas}}{N_{bats} V_{gas}} \right\|_2 + \beta_4 \left\| \frac{V_{dc}(N) - \bar{V}_{dc}}{\bar{V}_{dc}} \right\|_2 \right\} \quad (14b)$$

When the voltage level of battery is less than the threshold value of voltage level of the battery (gassing voltage), the proposed controller selects equation (14a) to charge the battery bank with the constant current  $I_c$ . Once the voltage level of battery exceeds the threshold value of voltage, the proposed controller selects equation (14b) to maintain it below the gassing voltage level of battery  $V_{gas}$  and thus guard batteries from occurring over charging which can cause permanent damages to the battery banks. In the above two

equations,  $\beta_1, \beta_2, \beta_3, \beta_4$  are the weight functions where the values of  $\beta_1$  and  $\beta_3$  are close to 1.0 and the values of  $\beta_2$  and  $\beta_4$  are close to zero.

Wind turbine	PMSG
$C_1(-)$	0.517
$C_2(-)$	116.0
$C_3(-)$	0.4
$C_4(-)$	5.0
$C_5(-)$	21.0
$C_6(-)$	0.007
$\lambda_{opt}(-)$	8.1
$P_{wt,nom}(KW)$	10.0
$Rad$ (m)	4.01
$U_{x,base}(m/s)$	12.0
$C_{p,max}(-)$	0.48
$J(Kg.m^2)$	0.35
$F(N.m.s)$	0.002
$P(-)$	8
$\psi(V.s)$	0.8
$P_{rated}(KW)$	10.0
$L_s(H)$	0.0083

TABLE 2(a) : WIND TURBINE & PMSG PARAMETERS IN THIS STUDY

Battery stack	PV array
$C_{max}(Ah)$	48.15
$R_{bat}(\Omega)$	0.019
$V_0(V)$	12.3024
$P_1(-)$	0.9
$N_{bats}(-)$	8
$N_{batp}(-)$	3
$T_s(sec)$	0.726
$V_{bstack,nom}(V)$	96.0
$P_{bat,nom}(KW)$	1.296
$C_{10}(Ah)$	45.0
$V_{gas}(V)$	13.0
$R_s(\Omega)$	0.221
$R_{sh}(\Omega)$	405.4
$n_d(-)$	1.3
$N_s(-)$	54
$I_{sc,stc}(A)$	8.21
$V_{oc,stc}(V)$	32.9
$k_I(A/K)$	0.003
$k_V(V/K)$	-0.12
$N_{pvs}(-)$	1
$N_{pvp}(-)$	10
$P_{pv,nom}(KW)$	2.001

TABLE 2(b) : BATTERY STACK & PHOTOVOLTAIC PARAMETERS IN THIS STUDY

#### IV. SIMULINK MODEL FOR THE PROPOSED SYSTEM

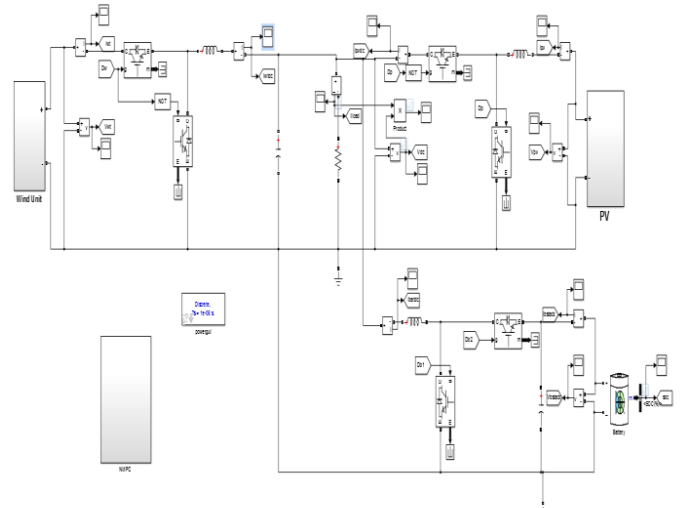


Fig.4. Simulink model for the proposed system

#### V. SIMULATION RESULTS AND DISCUSSIONS

The following graphs shows the simulation results that are obtained by using the proposed energy management strategy. i.e., by using NMPC technique.

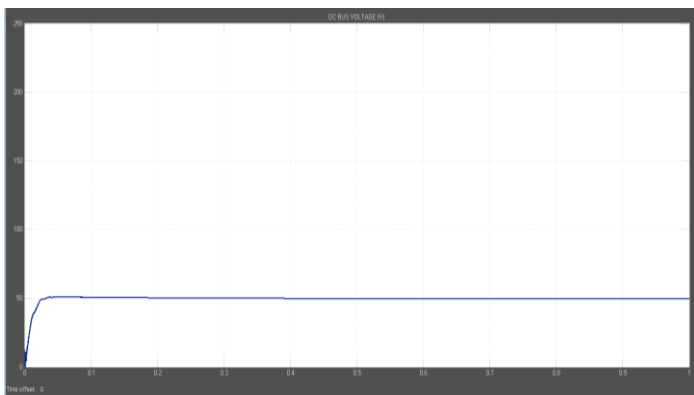


Fig.5. DC bus voltage level (V<sub>dc</sub>) in (Volts)

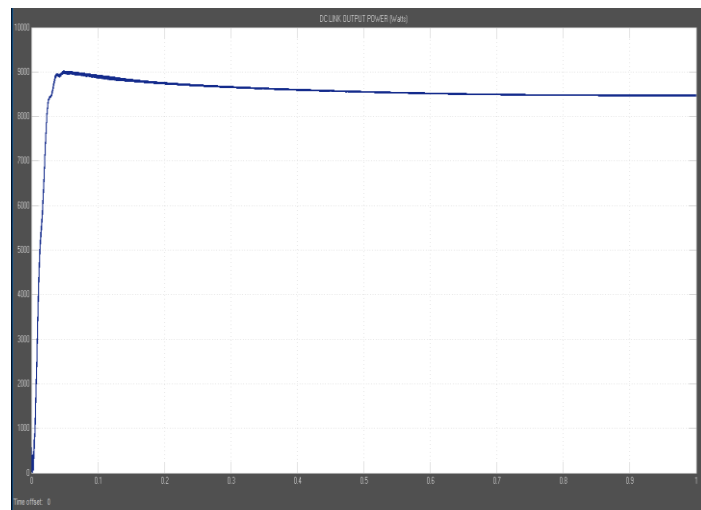


Fig.8. Total DC link output power (Watts)

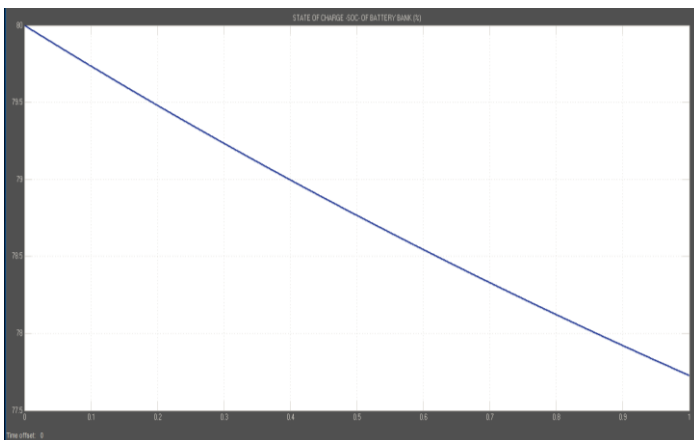


Fig.6. SOC of battery bank (discharging mode operation)in %

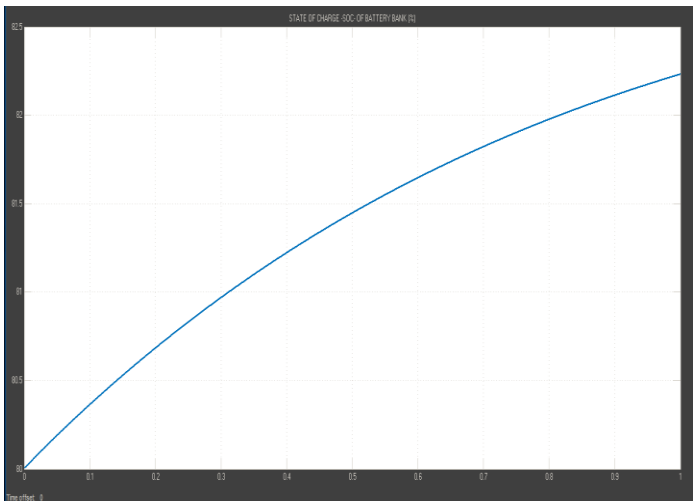


Fig.7. SOC of battery bank (charging mode operation) in %

In fig.5, the graph shows the DC bus voltage level as about 48V that we are giving. It can be identified that there is no distortions in the voltage we are giving. So the DC bus voltage regulation is done by the proposed NMPC method. The next figure ie., Fig.6 shows the state of charge (SOC) of the battery during the discharging mode operation. The charge in the battery bank is decreasing from about 80%. Fig.7 implies the battery operation during the charging mode. Battery charge is gradually increasing from 80% as shown in the graph. The last figure (Fig.8) is the total DC link output power graph. The power obtained here is about 8.5 KW. The NMPC control algorithm that we use here yields better output power of about 8.5KW compared to MPPT technique.

## VI . CONCLUSION AND FUTURE WORKS

This work consists of a study on modelling, simulation and control of standalone dc microgrids for the purpose of developing energy management technique. It can be identified that by employing latest available nonlinear optimization techniques and tools, the computational time to resolve the resulting NMPC strategy can be reduced. The proposed method can protect the battery from overcharging through the constant voltage and constant current charging method that can help to increase their life span. It is shown that the energy management methods are non linear multivariable optimal control problems. This work involves formulating optimal control problems and finding non linear model predictive control strategies to manage energy flows across stand-alone dc microgrids. The simulation results show its ability to achieve all control objectives.

## REFERENCES

- [1] J. M. Guerrero, M. Chandorkar, T. Lee, and P. C. Loh, "Advanced Control Architectures for Intelligent Microgrids-Part I: Decentralized and Hierarchical Control," *IEEE Trans. Ind. Electron.*, vol. 60, no. 4, pp. 1254–1262, 2013.
- [2] R. S. Balog, W. W. Weaver, and P. T. Krein, "The load as an energy asset in a distributed DC smartgrid architecture," *IEEE Trans. Smart Grid*, vol. 3, no. 1, pp. 253–260, 2012.
- [3] J. M. Guerrero, P. C. Loh, T. L. Lee, and M. Chandorkar, "Advanced Control Architectures for Intelligent Microgrids-Part II: Power quality, energy storage, and AC/DC microgrids," *IEEE Trans. Ind. Electron.*, vol. 60, no. 4, pp. 1263–1270, 2013.

[4] N. Eghtedarpour and E. Farjah, "Control strategy for distributed integration of photovoltaic and energy storage systems in DCmicrogrids," *Renew. Energy*, vol. 45, no. 0, pp. 96–110, 2012.

[5] D. Chen and L. Xu, "Autonomous DC voltage control of a DC microgrid with multiple slack terminals," *IEEE Trans. Power Syst.*, vol. 27, no. 4, pp. 1897–1905, Nov. 2012.

[6] L. Xu and D. Chen, "Control and operation of a DC microgrid with variable generation and energy storage," *IEEE Trans. Power Del.*, vol. 26, no. 4, pp. 2513–2522, Oct. 2011.

[7] S. Anand, B. G. Fernandes, and M. Guerrero, "Distributed control to ensure proportional load sharing and improve voltage regulation in low-voltage DC microgrids," *IEEE Trans. Power Electro.*, vol. 28, no. 4, pp. 1900–1913, 2013.

[8] B. Zhao, X. Zhang, J. Chen, C. Wang, and L. Guo, "Operation optimization of standalone microgrids considering lifetimecharacteristics of battery energy storage system," *IEEE Trans. Sustain. Energy*, to be published.

[9] T. Zhou and B. Francois, "Energy management and power control of a hybrid active wind generator for distributed power generation and gridintegration," *IEEE Trans. Ind. Electron.*, vol. 58, no. 1, pp. 95–104, 2011.

[10] X. Liu, P. Wang, and P. C. Loh, "A hybrid AC/DC microgrid and its coordination control," *IEEE Trans. Smart Grid*, vol. 2, no. 2, pp. 278–286, 2011.

[11] H. Kanchev, D. Lu, F. Colas, V. Lazarov, and B. Francois, "Energy management and operational planning of a microgrid with a PV-based active gen. for smart grid applications," *IEEE Trans. Ind. Electron.*, vol. 58, no. 10, pp. 4583–4592, 2011.

[12] H. Ghoddami, M. B. Delghavi, and A. Yazdani, "An integrated windphotovoltaic- battery system with reduced power-electronic interface and fast control for grid-tied and off-grid applications," *Renew. Energy*, vol. 45, no. 0, pp. 128–137, 2012.

[13] J.M. Guerrero, J. C. Vasquez, J.Matas, L. G. de Vicua, and M. Castilla, "Hierarchical control of droop-controlled AC and DC microgrids-a general approach toward standardization," *IEEE Trans. Ind. Electron.*, vol. 58, no. 1, pp. 158–172, 2011.

[14] P. H. Divsalar, A. Alimardani, S. H. Hosseinian, and M. Abedi, "Decentralized cooperative control strategy of microsources for stabilizing autonomous VSC-Based microgrids," *IEEE Trans. Power Syst.*, vol. 27, no. 4, pp. 1949–1959, Nov. 2012.

[15] P.C.Loh,D. Li, Y. K. Chai, and F.Blaabjerg, "Autonomous operation of hybrid microgrid with AC and DC subgrids," *IEEE Trans. Power Electron.*, vol. 28, no. 5, pp. 2214–2223, 2013.

[16] T. L. Vandoorn, B. Meersman, L. Degroote, B. Renders, and L. Vandeveld, "A control strategy for islanded microgrids with DC-Link voltage control," *IEEE Trans. Power Del.*, vol. 26, no. 2, pp. 703–713, Apr. 2011.

[17] T. L. Vandoorn, B. Meersman, J. D. M. De Kooning, and L. Vandeveld, "Analogy between conventional grid control and islanded microgrid control based on a globalDC-Link voltage droop," *IEEE Trans. Power Del.*, vol. 27, no. 3, pp. 1405–1414, Jul. 2012.

[18] H.Kakigano, Y. Miura, and T. Ise, "Distribution voltage control for DC microgrids using fuzzy control and gain-scheduling technique," *IEEE Trans. Power Electron.*, vol. 28, no. 5, pp. 2246–2258, 2013.

[19] H. Fakham, D. Lu, and B. Francois, "Power control design of a battery charger in a hybrid active PV generator for load-following applications," *IEEE Trans. Ind. Electron.*, vol. 58, no. 1, pp. 85–94, 2011.

[20] A.M. Dizqah, A.Maheri, K. Busawon, and P. Fritzson, "Acausal modeling and dynamic simulation of the standalone wind-solar plant using modelica," in *Proc. 2013 15th Int. Conf. ComputerModelling and Simulation (UK-Sim)*, 2013, pp. 580–585.

[21] A. Meharrar, M. Tioursi, M. Hatti, and A. B. Stambouli, "A variable speed wind generator maximum power tracking based on adaptative neuro-fuzzy inference system," *Expert Syst. Applicat.*, vol. 38, no. 6, pp. 7659–7664, 2011.

[22] H. Li and Z. Chen, "Overview of different wind generator systems and their comparisons," *IET Renew. Power Gener.*, vol. 2, no. 2, pp. 123–138, 2008.

[23] T. Burton, N. Jenkins, D. Sharpe, and E. Bossanyi, *Wind Energy Handbook*, 2nd ed. New York, NY, USA: Wiley, 2011.

[24] S. Heier, *Grid Integration of Wind Energy Conversion Systems*. New York, NY, USA: Wiley, 1998.

[25] N. Mohan, T. M. Undeland, and W. P. Robbins, *Power Electronics: Converters, Applications, and Design*. New York, NY, USA: Wiley, 1995.

[26] O. Tremblay and L. Dessaing, "Experimental validation of a battery dynamic model for EV applications," *World Elect. Vehicle J.*, vol. 3, pp. 10–15, 2009.

[27] J. J. Soon and K. S. Low, "Photovoltaic model identification using particle swarm optimization with inverse barrier constraint," *IEEE Trans. Power Electron.*, vol. 27, no. 9, pp. 3975–3983, 2012.

[28] M. G. Villalva, J. R. Gazoli, and E. R. Filho, "Comprehensive approach to modeling and simulation of photovoltaic arrays," *IEEE Trans. Power Electron.*, vol. 24, no. 5, pp. 1198–1208, 2009.